www.sciencemag.org/cgi/content/full/325/5947/1541/DC1

Supporting Online Material for

A Constant Flux of Diverse Thermophilic Bacteria into the Cold Arctic Seabed

Casey Hubert,* Alexander Loy, Maren Nickel, Carol Arnosti, Christian Baranyi, Volker Brüchert, Timothy Ferdelman, Kai Finster, Flemming Mønsted Christensen, Júlia Rosa de Rezende, Verona Vandieken, Bo Barker Jørgensen

*To whom correspondence should be addressed. E-mail: chubert@mpi-bremen.de

Published 18 September 2009, *Science* **325**, 1541 (2009)
DOI: 10.1126/science.1174012

This PDF file includes:

Supporting Online Material

A Constant Flux of Diverse Thermophilic Bacteria into the Cold Arctic Seabed

Casey Hubert, Alexander Loy, Maren Nickel, Carol Arnosti, Christian Baranyi, Volker Brüchert, Timothy Ferdelman, Kai Finster, Flemming Mønsted Christensen, Júlia Rosa de Rezende, Verona Vandieken, and Bo Barker Jørgensen

---

Materials and Methods

Location and sampling. Marine sediment was sampled during research cruises to Svalbard fjords aboard R/V *Farm* during summer months of 2003 to 2006. Smeerenburgfjorden is situated on the northwest coast of Svalbard (79°43'N, 11°05'E; see fig. S1) and the water depth at our sampling station is 210 m. Surface sediment (0-10 cm) was also sampled from Magdalenefjorden (79°34'N, 11°04'E), Kongsfjorden (78°55'N, 12°16'E), Nordfjorden (78°31'N, 15°04'E), Isfjorden (78°11'N, 14°34'E) and van Mijenfjorden (77°46'N, 15°04'E), as indicated in fig. S1. Sediments were obtained using a Haps corer (Kanneworf and Nicolaisen, 1983) with a 120 mm diameter core liner, allowing ship board sub-sampling into cores or gas-tight plastic bags (Hansen *et al*., 2000) for incubation experiments. A longer Rumohr gravity corer (Meischner and Rumohr, 1974) was used to obtain a 36 cm deep core from Smeerenburgfjorden that was cut into 2 cm sections to determine the sediment accumulation rate at this site.

Temperature gradient incubations. A sediment slurry (1:2 w/w) was prepared by mixing surface sediment with anoxic synthetic seawater (Widdel and Bak, 1991) and amended with volatile fatty acids (VFA). After overnight stirring at 4°C under N_2, aliquots (10 ml) were transferred to Hungate tubes and sealed with rubber stoppers. Tubes were incubated in temperature gradient blocks (TGB), which were 200×15×15 cm insulated aluminum blocks cooled at one end and

heated at the other to create a gradient from 0° to 76°C that increased incrementally between incubation slots. Half of the tubes were pasteurized in an 80°C water bath for one hour then immediately transferred to the TGB. Following pre-incubation in the TGB, 100 to 500 kBq of anoxic ^{35}S-labeled sulfate radiotracer solution was added to each tube. Sulfate reduction was terminated 4 to 8 hours later by transferring slurries into 20 ml zinc acetate solution (20% w/v) and freezing. Sulfate reduction rates (SRR) were determined by cold chromium distillation according to Kallmeyer *et al*. (2004). Triplicate slurries were incubated at several experimental temperatures resulting in standard deviations that were on average 12.7% of mean SRR.

Homogenized sediment incubations at 4° and 50°C. Bags of anoxic Smeerenburgfjorden sediment collected from 0 to 3 cm depth were incubated at 4° and 50°C with sub-samples removed for pore water analyses and determining SRR after 0, 8, 16, 24, 48, 72 and 96 h. Pore water was obtained from homogenized sediment sub-samples with a pore water press under N_2 pressure through GF/F filters. For SRR, sediment was dispensed into 10×1 cm cylindrical glass tubes that were sealed with a rubber stopper at one end and with a plastic syringe piston at the other end. Approximately 100 kBq of anoxic radiotracer solution was injected into the glass tubes, which then incubated at 4° or 50°C in parallel with the ongoing sediment bag incubations. Sulfate reduction was terminated 4 to 8 hours later (end-point times as listed above). Rates and concentrations determined at time zero for the bag incubated near in situ temperature (4°C) were inferred as initial data (time zero) for the 50°C incubation. For incubations at 50°C involving amendments with organic substrates, sediment slurries (1:2 w/w) were used. Thermophilic strains were isolated at 50°C by dilution to extinction in media inoculated with Smeerenburgfjorden sediment, followed by successive transfers in agar shake tubes.

Intact sediment core incubations. Sediment sub-cores (26 mm diameter) were taken from intact Haps cores immediately after retrieval. Replicate cores were incubated at 50°C and duplicate cores were removed on a daily basis (at similar

times as for the bag incubations). Radiotracer was injected for the final 4 to 8 hours of incubation, after which sulfate reduction was stopped and SRR were determined.

Analytical methods. Pore water was extracted regularly from sediment incubations for various analyses. Concentrations of VFA were measured by UV absorbance at 400 nm after derivitization with p-nitrophenyl hydrazine (Albert and Martens, 1987; Finke and Jørgensen, 2008). Hydrolytic potential was determined by amending sediment slurries with fluorescently labelled polysaccharides and analysing hydrolysis rates in 50°C incubations using gel permeation chromatography (Arnosti, 2003) relative to thermal controls (the same polysaccharides incubated at 50°C without sediment). Dissolved inorganic carbon (DIC) was determined by fixing 1.8 ml porewater aliquots with 20 µl of saturated $HgCl_2$ solution in glass vials capped with Viton septa without headspace. These were stored at 4°C until analysis by flow injection with conductivity detection (Hall and Aller, 1992). For ammonium analyses 1.5 ml aliquots were stored frozen prior to spectrophotometric determination with indophenol at 630 nm (Grasshoff *et al*., 1999). Porewater for sulfate analyses was preserved with zinc acetate (2% w/v) and measured by non-suppressed ion chromatography (Waters, column IC-PakTM, 50 x 4.6 mm) and conductivity detection using sodium phthalate eluent, pH 4.7, buffered with sodium tetraborate (Ferdelman *et al*., 1997).

16S rRNA gene surveys and phylogenetic analysis. DNA was extracted from sediment before and after incubation at 50°C using a previously described protocol (Zhou *et al*., 1996) or the Power Soil kit (MoBio). The presence of *Desulfotomaculum* was tested for using genus-specific 16S rRNA gene-targeted primers (116F and 1164R) (Stubner and Meuser, 2000). For clone libraries, bacterial 16S rRNA gene products obtained with PCR primers 8F and 1492R were cloned using the Topo TA cloning kit (Invitrogen). Taq cycle sequencing of clones was performed with an ABI3130xl sequencer (Applied Biosystems). After removing chimeras, 16S rRNA gene sequences (*E. coli* positions 100-1380) with identities ≥99% (approximately defining species level phylotypes; Stackebrandt

and Ebers, 2006) were grouped in operational taxonomic units (OTUs/phylotypes) using the furthest neighbour algorithm of DOTUR (Schloss and Handelsman, 2005). Treeing was performed using a 50% conservation filter for *Bacteria*, and the neighbour-joining, maximum-likelihood and maximum-parsimony methods in ARB (Ludwig *et al*., 2004). Polytomies were introduced in the consensus tree when branching patterns were inconsistent for the different trees. Two maximum likelihood trees (AxML, PHYML) of all clone sequences (n=181) were used for unweighted UniFrac analysis (Lozupone *et al*., 2006) to determine differences in the composition of bacterial communities before and after incubation at 50°C.

Determination of excess ^{210}Pb activity. The distribution of excess ^{210}Pb activity in a Rumohr core obtained from Smeerenburgfjorden was used to constrain sediment burial rates. Unsupported (excess) ^{210}Pb activity was calculated as the difference between total ^{210}Pb activity and ^{210}Pb supported by in situ ^{226}Ra decay. ^{226}Ra was determined as the activity of its short-lived daughter products ^{214}Pb and ^{214}Bi. Freeze-dried sediment samples (4 to 19 grams) obtained at 2 cm sediment depth intervals were stored in polysulfone screw-top jars (diameter 45 mm) and kept for at least 20 days in order that secular equilibrium between the parent isotope ^{226}Ra and short-lived daughter products ^{222}Rn, ^{214}Pb, and ^{214}Bi was reached. Activities were determined by non-destructive gamma spectroscopy using an ultra-low-level germanium gamma detector (Canberra, EURISYS coaxial type N). Depending on the expected activity, individual samples were counted for 1 to 4 days. Activities of the isotopes ^{210}Pb (46.4 keV), ^{214}Pb (295.2 and 352 keV) and ^{214}Bi (609.3 keV) were corrected for detector efficiency and intensity obtained from calibration with a uranium-thorium ore reference standard (DL-1a, Canadian Certified Reference Materials Project). ^{210}Pb self-absorption was checked individually for every sample (Cutshall *et al*., 1983) using a 10 kBq ^{210}Pb source (AEA Technology). ^{137}Cs and ^{40}K were additionally quantified at the 667 keV and 1460 keV lines respectively.

Supporting Online Text (Results and Discussion)

Svalbard. A map indicating our main sampling location in Smeerenburgfjorden is shown in fig. S1. Incubations at 50°C were also performed with sediment from other locations along the west coast of Svalbard (described below and shown in fig. S1).

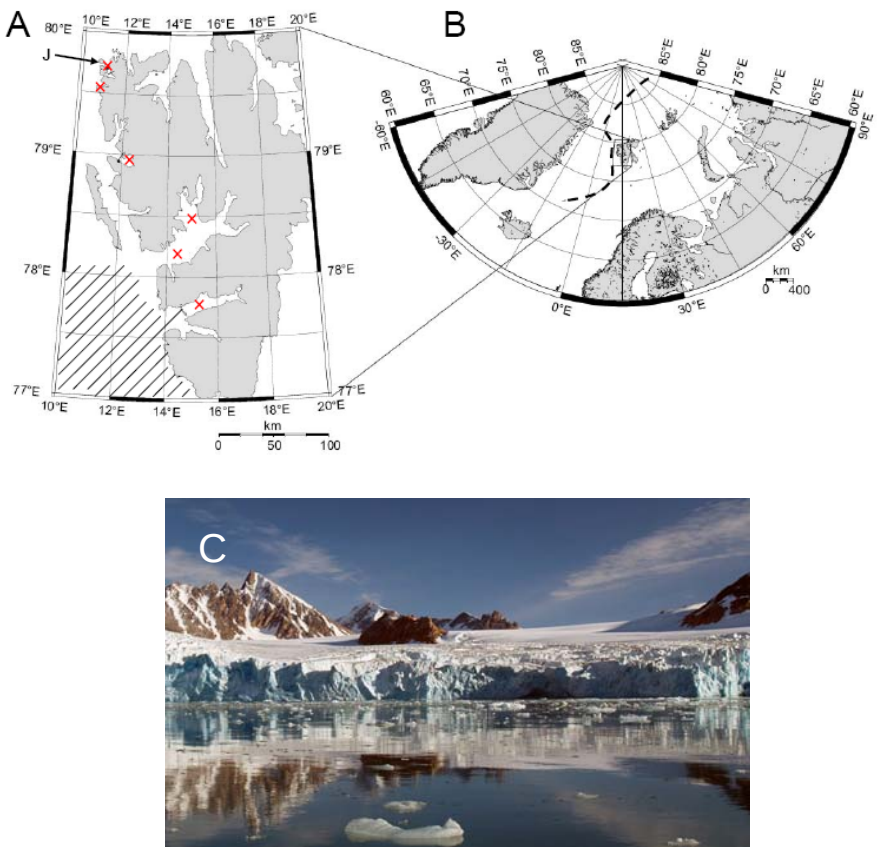

Figure S1. Svalbard fjords. The main sediment sampling location was station J in Smeerenburgfjorden (C) located at 79°43'N, 11°05'E ("J" indicated by the arrow in A). Sediment in Smeerenburgfjorden and other Svalbard fjords is permanently cold with year round in situ temperatures between –2° and +4°C. Exponential increases in SRR were observed in 50°C incubations with sediment from several locations, which are indicated (×) in (A) and correspond to estimated in situ densities of thermophilic SRB >10^4 cm^{-3} (see SOM Text below). The northern extent of a recent study of submarine gas seepage (Damm *et al*., 2005) is indicated by the diagonal lines in (A). The approximate location of the mid-ocean spreading ridge is indicated by the dashed line (B).

Estimating thermophilic *Desulfotomaculum* abundance in Svalbard sediments. Estimating thermophilic SRB abundance in heated sediments depends on an exponential increase in SRR. This can be described by a function that allows the rate at the beginning of this increase to be extrapolated. In our main 50°C incubation experiment (Fig. 2A) this was 1.3 nmol cm^{-3} $hour^{-1}$ after 16 hours. The exponential response is presumably catalyzed by a growing SRB population that reduces sulfate at a constant cell-specific sulfate reduction rate (cs-SRR). Detmers *et al*. (2001) reported cs-SRR values for 33 pure cultures during exponential growth, and we used their mean value (2.0 fmol $cell^{-1}$ $hour^{-1}$) to estimate 6.3×10^5 SRB cm^{-3} present at 16 hours. Among the 33 pure cultures analyzed, thermophilic *Desulfotomaculum* spp. had cs-SRR values near the maximum and minimum reported (Detmers *et al*., 2001). *Desulfotomaculum geothermicum* – isolated from geothermal groundwater (Daumas *et al*., 1988) and the closest described relative to the thermophilic *Desulfotomaculum* lineage we detected in Smeerenburgfjorden – has a cs-SRR of 0.3 fmol $cell^{-1}$ h^{-1} (Detmers *et al*., 2001); for the data in Fig. 2A this results in a higher in situ SRB density estimate of 4.3×10^6 spores cm^{-3} (fig. S2). On the other hand, Detmers *et al*. (2001) report a high cs-SRR of 12.9 fmol $cell^{-1}$ $hour^{-1}$ for *Desulfotomaculum thermocisternum* (from a hot North Sea oil reservoir; Nilsen *et al*., 1996), which when applied here gives a lower estimate of 1.0×10^5 spores cm^{-3} in situ (fig. S2). The mean cs-SRR value therefore represents the range for thermophilic *Desulfotomaculum*. This range is indicated in the depth profile in fig. S2. Dilution to extinction experiments were performed by inoculating pasteurized sediment into growth medium amended with VFA. These provided minimum estimates of the most probable number (MPN) of thermophilic SRB in the range of 10^1 to 10^2 cm^{-3} in the Arctic and 10^1 to 10^4 cm^{-3} in temperate sediments (Isaksen *et al*., 1994). This confirmed the presence of thermophilic spores, yet for all sediments tested MPN counts were lower than the minimum estimate using cs-SRR (i.e., applying 12.9 fmol $cell^{-1}$ $hour^{-1}$). The MPN approach is known to underestimate actual numbers by several orders of magnitude (Sahm *et al*., 1999), as is evident here given the extremely high cs-SRR required for an in situ SRB density much below 10^5 cm^{-3} (Fig. 2A; fig. S2).

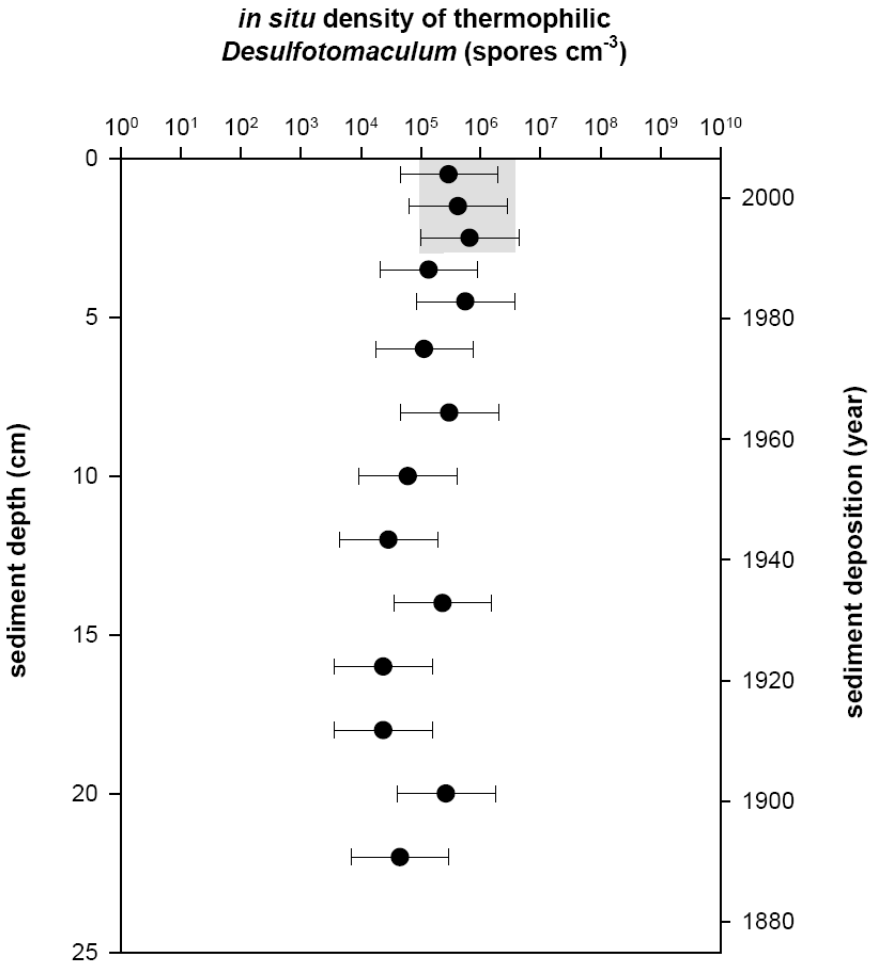

Figure S2. Depth distribution of *Desulfotomaculum* spores. The in situ abundance of thermophilic SRB was estimated from exponential increases in sulfate reduction rates (SRR) measured in intact sediment cores incubated at 50°C (table S1). Plotted values were estimated using a mean cs-SRR as described in the SOM Text. Horizontal bars indicate minimum and maximum cell density estimates based on cs-SRR values reported for thermophilic *Desulfotomaculum* spp. (Detmers *et al*., 2001) as described in the SOM Text. The same estimate for the 0-3 cm sediment incubation (Fig. 2A) is indicated by the shaded area and agrees with estimates from the sediment cores. A sediment age model for Smeerenburgfjorden determined from excess ^{210}Pb activity as a function of depth (see SOM Text and fig. S4) is shown on the right y-axis and corresponds to a sediment accumulation rate of 0.19 cm year^{-1}.

Estimating thermophilic SRB abundance in other Svalbard sediments. Slurries prepared with surface sediment from Magdalenefjorden, Kongsfjorden, Isfjorden, Nordfjorden and van Mijenfjorden (fig. S1) were amended with VFA and sulfate radiotracer. Incubation at 50°C resulted in exponential increases in sulfate reduction, allowing estimates of thermophilic SRB abundance in situ, which were $>10^4$ cm^{-3} in each sediment (based on the approach outlined above). This confirms that our observations are not unique to Smeerenburgfjorden.

Microbial activity at 4° and 50°C in sediment incubations. Bags of homogenized sediment (ca. 1 kg) were incubated at 4° and 50°C. Sulfate reduction rates (SRR) at 4°C were always 5-9 nmol cm^{-3} $hour^{-1}$ (fig. S3A). This is slightly higher than in situ SRR (table S1), which is attributed to enhanced organic substrate availability for microbial metabolism in homogenized sediment (Hansen *et al*., 2000). At 50°C SRR increased exponentially to levels much higher than those measured at 4°C (fig. S3A, B). As described in the Main Text, hydrolysis and fermentation in the early hours of 50°C incubations preceded the sulfate reduction phase (Fig. 2). This is evident from comparing DIC and ammonium plots with the plot of SRR for the 50°C incubation (fig. S3B, D, F). Production of 5 mM DIC in the first 24 hours did not correspond to any sulfate reduction; however subsequent production of 15 mM DIC (24-96 hours) coincided with thermophilic SRB activity. Ammonium concentrations increased most rapidly during the first 24 hours of the 50°C incubation (fig. S3F), coinciding with the period of rapid VFA production (Fig. 2B). Small changes in DIC and ammonium were observed in sediments incubated at 4°C (fig. S3C, E).

Sulfate reduction in sediment core incubations. Replicate sub-cores from Smeerenburgfjorden were incubated at 4° and 50°C. In situ SRR were determined at 4°C and are shown in table S1. In the 50°C experiment SRR were determined at 1-2 cm intervals during a time-course similar to the bag incubation with homogenized sediment (Fig. 2A; fig. S3B). Functions describing exponential increases in sulfate reduction at each depth are shown in table S1 and were used to estimate initial spore numbers (as described in the Main Text and SOM Text and plotted in fig. S2).

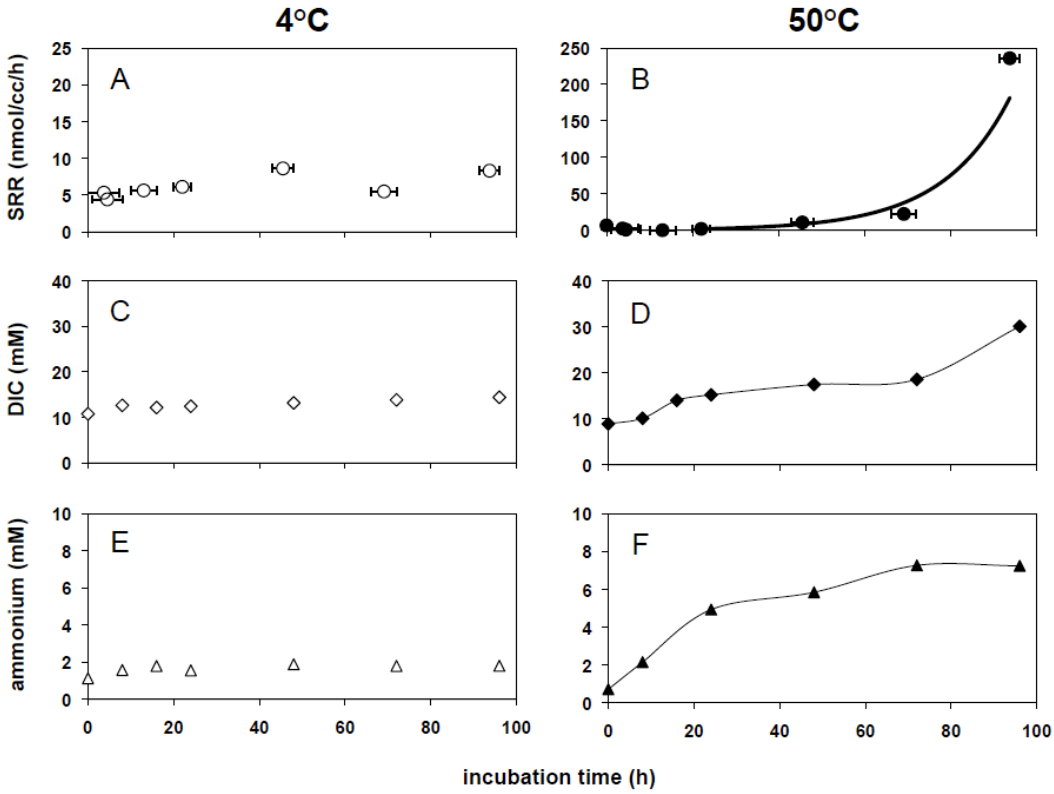

Figure S3. Time course bag incubations. Smeerenburgfjorden sediment (from 0 to 3 cm depth) was incubated in anoxic bags at 4°C (A, C, E) and 50°C (B, D, F). SRR (A, B) and concentrations of DIC (C, D) and ammonium (E, F) were monitored as a function of incubation time. The data and trendline for SRR at 50°C (B) are re-plotted from Fig. 2A for comparison purposes.

Table S1. Sulfate reduction at 50° and 4°C in different sediment depths.

Depth (cm)	SRR at 50°C ($ae^{b(t)}$)	R^2	interval[a]	$SRR_{onset.}$ [b]	in situ SRR[c]
0-1	$0.207\, e^{0.064(t)}$	0.98	24-86 h	0.58	0.53
1-2	$0.251\, e^{0.075(t)}$	0.91	48-86 h	0.83	1.12
2-3	$0.416\, e^{0.071(t)}$	0.99	48-86 h	1.30	2.51
3-4	$0.063\, e^{0.090(t)}$	0.90	48-86 h	0.27	1.70
4-5	$0.459\, e^{0.055(t)}$	0.92	48-104 h	1.11	1.91
5-7	$0.068\, e^{0.075(t)}$	0.94	48-104 h	0.23	1.98
7-9	$0.240\, e^{0.057(t)}$	0.94	48-104 h	0.60	1.03
9-11	$0.045\, e^{0.062(t)}$	0.94	68-124 h	0.12	0.26
11-13	$0.019\, e^{0.068(t)}$	0.97	68-124 h	0.06	0.30
13-15	$0.245\, e^{0.039(t)}$	0.95	68-124 h	0.46	0.99
15-17	$0.020\, e^{0.054(t)}$	0.99	86-124 h	0.05	0.58
17-19	$0.019\, e^{0.057(t)}$	0.96	86-124 h	0.05	0.69
19-21	$0.259\, e^{0.044(t)}$	0.98	48-86 h	0.52	0.76
21-23	$0.039\, e^{0.052(t)}$	0.82	68-124 h	0.09	0.66
0-3 (bag)	$0.454\, e^{0.064(t)}$	0.97	20-96 h	1.26	6.82[d]

[a] Exponentially increasing SRR were measured during these intervals in 50°C incubations.

[b] The sulfate reduction rate (nmol cm^{-3} $hour^{-1}$) extrapolated to the onset of the exponential phase (i.e., after 16 hours, as described in the SOM Text).

[c] Mean sulfate reduction rate (nmol cm^{-3} $hour^{-1}$) from duplicate cores incubated at 4°C.

[d] Mean sulfate reduction rate during the 4°C bag incubation (fig. S3A).

16S rRNA gene surveys and phylogenetic analysis. Clone libraries were constructed before (time zero) and after (56 hours) incubation at 50°C. Good's coverage for the two libraries was 46% and 65%, respectively (table S2). Both p-test and UniFrac significance testing showed that the two bacterial communities differed significantly (p-value <0.001). Lineage-specific UniFrac analysis (using approximately phylum level distance; Lozupone *et al*., 2006) indicated that only members of the phylum *Firmicutes* contributed significantly to this difference (p-value < 0.001). Out of 85 clone sequences in the 50°C sediment library, 40 grouped within the *Firmicutes* phylum (Fig. 3), as opposed to only one out of 96 clone sequences in the library constructed prior to incubation at 50°C. The low proportion of *Firmicutes* in the initial clone library agrees with previous in situ molecular community analyses of Svalbard fjord sediments (Ravenschlag et al., 1999; 2000; 2001). Phylotypes represented by 0 clones before, and >5% of clones following incubation at 50°C, were considered to represent Arctic thermophiles enriched at high temperature (indicated in Fig. 3 and table S3). To evaluate putative physiologies and possible sources of Arctic thermophiles, next relatives to these dominant phylotypes were determined using the SINA aligner of SILVA (Pruesse *et al*., 2007) and the sequence match option in RDP II (Cole *et al*., 2007) (Fig. 3 and table S3).

Table S2. Clone libraries before and after sediment incubation at 50°C.

Library designation	Before 50°C (0 h)	After 56 h at 50°C	Both
Number of clones	96	85	181
Number of OTUs	68	41	99
Number of singletons[a]	52	30	68
Good's Coverage	46%	65%	62%

[a] OTUs represented by only one sequence in the clone library

Table S3. *Firmicutes* enriched at 50°C and their closest relatives.

OTU[a]	Number of clones	Next relative (accession number), max. 16S rRNA identity
A	15 (18%)	Hypersaline microbial mat clone (EU245157), 94.5% [b]*Clostridiisalibacter* sp. SOL3f37 (EU567322), 93.6%
B	10 (12%)	[c]Gram positive thermophile ODP15902 (AY704384), 94.1%
C	4 (5%)	[d]North Sea Troll oil reservoir clone (DQ647124), 96% [e]*Caminicella sporogenes*^{T} (AJ320233), 94%
D	7 (8%)	Gas field formation fluid clone (EU999019), 95.7% [f]*Desulfotomaculum geothermicum*^{T} (Y11567), 95.6%

[a] OTU designations as indicated in Fig. 3.

[b] Isolated from petroleum contaminated soil at an oil production facility.

[c] Isolated from Juan de Fuca ridge flank crustal fluid (Huber *et al*., 2006); this strain was more closely related than any environmental clones in the databases (Fig. 3).

[d] Formation water from a high temperature oil reservoir (Dahle et al., 2008).

[e] Isolated from a hydrothermal vent site (Alain *et al*., 2002).

[f] Isolated from 2.5 km deep geothermal groundwater (Daumas *et al*., 1988).

Smeerenburgfjorden ^{210}Pb and estimation of sediment burial rate. Distributions of total ^{210}Pb and ^{226}Ra versus depth are shown in fig. S4A. Background activities of ^{226}Ra, and therefore of ^{226}Ra-supported ^{210}Pb, are constant at 2.2 ± 0.2 dpm cm^{-3}. ^{210}Pb activities decrease exponentially from a surface peak activity of 20.9 dpm cm^{-3} with increasing depth and approach the values of secular equilibrium with respect to ^{226}Ra of 2.2 at depths below 30 cm. The ^{210}Pb profile exhibits distinct deviations from a smooth exponential decrease. These deviations correlated with distinct shifts in the ^{40}K, porosity, and bulk density distributions (data not shown).

Reaction-transport models using unsupported (excess) ^{210}Pb (^{210}Pb$_{xs}$) to estimate sediment burial rates assume that sediment depth and age are equivalent, and that the flux of ^{210}Pb is known or at least constant over time (Robbins, 1978). Superficially, the Smeerenburgfjorden sediment does not appear to meet these criteria, given the variable sedimentation and sediment mixing caused by burrowing infauna. Changes in porosity, bulk sediment density and ^{40}K, along with the deviations in the ^{210}Pb$_{xs}$ profile suggest that the rate of sedimentation has varied over time. That is, variable and lateral inputs of glacier derived "^{210}Pb-old" sediments dilute the flux of ^{210}Pb$_{xs}$-bearing particles to the sediment-water interface. We assume that the flux of ^{210}Pb$_{xs}$ has remained constant over the past 100 years, but the rate of overall sediment input may have varied. The so-called constant flux model (Robbins, 1978) can be used to establish a sediment age model whereby the age for any given layer can be estimated from the following relationship:

$$t = \frac{1}{\lambda}\ln\left[1 - \frac{\Gamma_z}{\Gamma_\infty}\right]$$

where: t = age of bottom of layer z in years

λ = decay constant for ^{210}Pb = 0.0311 y^{-1}

Γ_z = inventory of ^{210}Pb$_{xs}$ below depth z

Γ_∞ = total inventory of ^{210}Pb$_{xs}$ in sediment

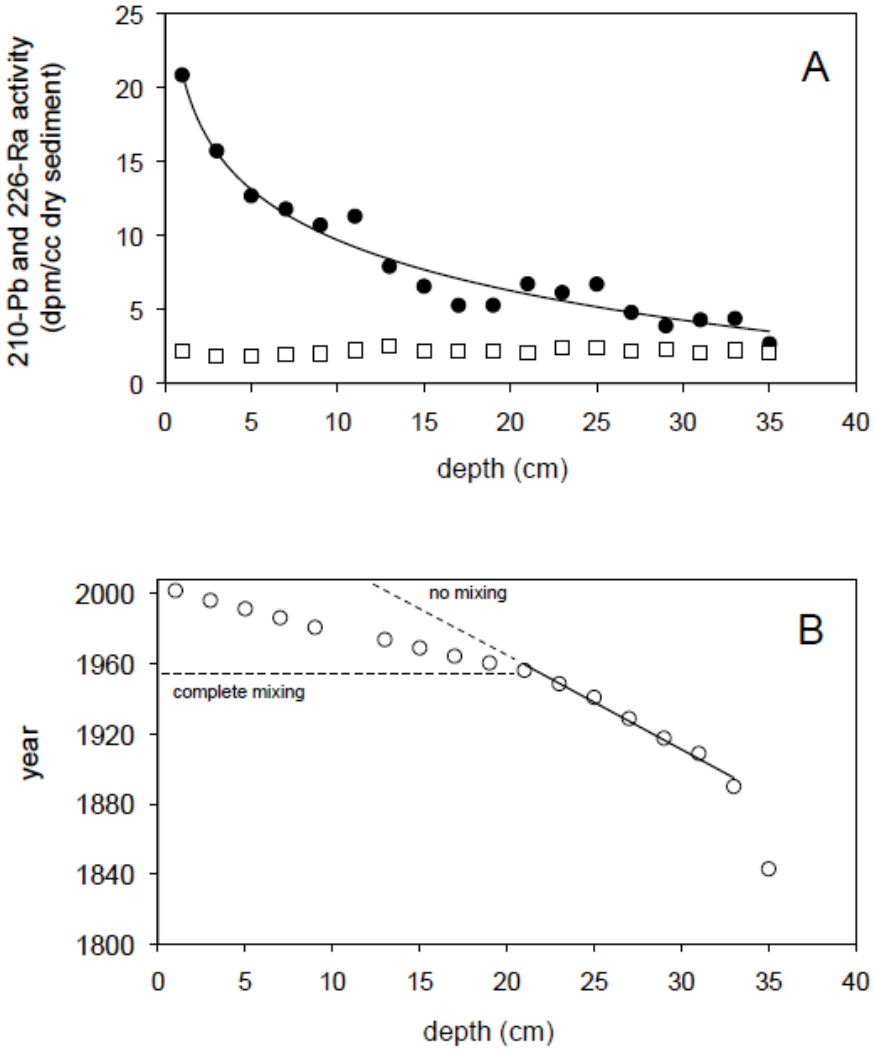

Figure S4. Depth profiles of ^{210}Pb and ^{226}Ra and sediment age model. Activities of total ^{210}Pb (●) and ^{226}Ra (□) measured in freeze-dried sediment (2 cm depth intervals) from Smeerenburgfjorden (A). The exponential decrease in ^{210}Pb activity displays some unevenness, indicating that the surface sediment (down to 20 cm) was partially, but not completely mixed by burrowing infauna (Jørgensen *et al*., 2005). From these data, unsupported (excess) ^{210}Pb activity was calculated and used in a constant flux model (Robbins, 1978) to construct a sediment age profile (B). The steeper slope below 20 cm depth (where there is no influence of bioturbation) allows a burial rate of 0.19 cm year^{-1} to be calculated for Smeerenburgfjorden.

Bioturbation in Smeerenburgfjorden sediments is assumed to be small enough not to violate entirely the assumption of depth-age equivalency. Qualitative observations (during core sectioning) of tube-dwelling polychaetes and other fauna are similar to those observed in surface sediments of other Svalbard fjords (Jørgensen *et al*., 2005). The $^{210}Pb_{xs}$ data for the top 20 cm indicate that bioturbation results only in partial mixing of this sediment layer, as decay still proceeds with depth (fig. S4A). The stable profile of *Desulfotomaculum* spore abundance down to 23 cm (fig. S2) is thus not a function of mixing (the sediment is not completely mixed; fig. S4B) and corresponds to a stable input of spores to the sediment. Mixing is assumed to approach zero below 20 cm, and data from this zone can be used to estimate a sediment burial rate of 0.19 cm $year^{-1}$ (fig. S4B).

References for Supporting Online Material

S1. E. Kanneworff, W. Nicolaisen, *Ophelia* **22**, 253 (1983)

S2. J. W. Hansen, B. Thamdrup, B. B. Jørgensen, *Mar. Ecol. Prog. Ser.* **208**, 273 (2000).

S3. D. Meischner, J. A. Rumohr, *Senckenbergiana marit*. **6**, 105 (1974).

S4. F. Widdel, F. Bak, in *The Prokaryotes 2nd Edition* (eds A. Balows, H. G. Trüper, M. Dworkin, W. Harder, K. H, Schleifer) **4**, 3352-3378 (Springer, New York, 1992).

S5. J. Kallmeyer, T. G. Ferdelman, A. Weber, H. Fossing, B. B. Jørgensen, *Limnol. Oceanogr. Meth.* **2**, 171 (2004).

S6. D. B. Albert, C. S. Martens, *Mar. Chem* **56**, 27 (1997).

S7. N. Finke, B. B. Jørgensen, *ISME J.* **2**, 815 (2008).

S8. C. Arnosti. *J. Chromatog. B.* **793**, 181 (2003).

S9. P. O. J. Hall, R. C. Aller, *Limnol. Oceanog.* **37**, 1113 (1992).

S10. K. Grasshoff, K. Kremling, M. Ehrhardt, in *Methods of seawater analysis* (Wiley, Weinheim, 1999).

S11. T. G. Ferdelman *et al*. *Geochim. Cosmochim. Acta* **61**, 3065 (1997).

S12. J. Zhou, M. A. Bruns, J. M. Tiedje, *Appl. Environ. Microbiol.* **62**, 316 (1996).

S13. S. Stubner, K. Meuser, *FEMS Microbiol. Ecol*. **34**, 73 (2000).

S14. E. Stackebrandt, J. Ebers, *Microbiol. Today* November (2006).

S15. P. D. Schloss, J. Handelsman, *Appl. Environ. Microbiol*. **71**, 1501 (2005).

S16. W. Ludwig *et al*., *Nuc. Acids Res*. **32**, 1363 (2004).

S17. C. Lozupone, M. Hamady, R. Knight, *BMC Bioinf*. **7**, 371 (2006).

S18. N. H. Cutshall, I. L. Larsen, C. R. Olsen, *Nucl. Inst. Meth. Phys. Sec. A*. **206**, 309 (1983).

S19. E. Damm, A. Mackensen, G. Budéus, E. Faber, C. Hanfland, *Cont. Shelf. Res.* **25**, 1453 (2005).

S20. J. Detmers, V. Brüchert, K. S. Habicht, J. Kuever, *Appl. Environ. Microbiol*. **67**, 888 (2001).

S21. S. Daumas, R. Cord-Ruwisch, S. L. Garcia, *Ant. van Leeuw*. **54**, 165 (1988).

S22. R. K. Nilsen, T. Torsvik, T. Lien, *Int. J. Sys. Bact.* **46**, 397 (1996).

S23. M. F. Isaksen, F. Bak, B. B. Jørgensen, *FEMS Microbiol. Ecol*. **14**, 1 (1994).

S24. K. Sahm, B. J. MacGregor, B. B. Jørgensen, D. A. Stahl, *Environ. Microbiol*. **1**, 65 (1999).

S25. K. Ravenschlag, K. Sahm, J. Pernthaler, R. Amann, *Appl. Environ. Microbiol.* **65**, 3982 (1999).

S26. K. Ravenschlag, K. Sahm, C. Knoblauch, B. B. Jørgensen, R. Amann, *Appl. Environ. Microbiol.* **66**, 3592 (2000).

S27. K. Ravenschlag, K. Sahm, R. Amann, *Appl. Environ. Microbiol*. **67**, 387 (2001).

S28. E. Pruesse *et al*., *Nucl. Acid. Res*. **35**, 7188 (2007).

S29. J. R. Cole *et al*., *Nucl. Acid. Res*. **35**, D169 (2007).

S30. J. A. Huber, P. Johnson, D. A. Butterfield, J. A. Baross, *Environ. Microbiol*. **8**, 88 (2006).

S31. H. Dahle, F. Garshol, M. Madsen, N. K. Birkeland, *Anton. van. Leeuw*. **93**, 37 (2008).

S32. K. Alain *et al*., *Intl. J. Syst. Evol. Microbiol*. **52**, 1621 (2002).

S33. J. A. Robbins in *The Biogeochemistry of Lead in the Environment Part A* (ed. J. O. Nriagu) pp 285-393 (Elsevier, Amsterdam, 1978).

S34. B. B. Jørgensen, R. N. Glud, O. Holby, *Mar. Ecol. Prog. Ser*. **292**, 85 (2005).